Feng *et al. Robomech J* (2021) 8:10
https://doi.org/10.1186/s40648-021-00194-5

ROBOMECH Journal

RESEARCH ARTICLE Open Access

Safety-enhanced control strategy of a power soft robot driven by hydraulic artificial muscles

Yunhao Feng[1*], Tohru Ide[1], Hiroyuki Nabae[1], Gen Endo[1], Ryo Sakurai[2], Shingo Ohno[2] and Koichi Suzumori[1]

Abstract

Power soft robots—defined as novel robots driven by powerful soft actuators, achieving both powerfulness and softness—are potentially suitable for complex collaborative tasks, and an approach to actuating a power soft robot is the McKibben artificial muscle. This study aims to show the potential of hydraulic artificial muscles to be implemented in a power soft robot with high safety, including higher stability against sudden load separation or impact disturbance, and appropriate dynamic compliance. The stability of a manipulator arm driven by hydraulic muscle actuators is experimentally proven to be higher than that of pneumatic muscle actuators when the stored elastic energy is instantaneously released. Therefore, the hydraulic muscle actuator is a better candidate for actuating a power soft robot. By taking advantage of the incompressible liquid medium and the compliant structure of a hydraulic muscle, a second-order impedance control strategy with a braking method is proposed to improve dynamic compliance without sacrificing the safety features of hydraulic muscles. The results show that the manipulator can be easily shifted by a several-kilogram-level external force and react safely against sudden load change with low angular velocity by the proposed impedance control.

Keywords: Power soft robot, Hydraulic muscle actuator, Impedance control

Introduction

It is a general assumption that softness and powerfulness are contrasting concepts; however, they are actually independent and can be achieved simultaneously. The goal of our research is to develop a robot that has both properties: powerfulness and softness.

Traditional robots, which use stiff actuators with high power and high accuracy, have already been applied in many industries to accomplish heavy tasks. On the other hand, novel soft actuators have intrinsic compliance, which is particularly suitable for human–robot interaction. However, most of the current soft actuators lack power. For heavy tasks that require interaction with humans, when both high power and high compliance are required, traditional collaborative robots have to be equipped with other safety components and advanced control methods to increase compliance and safety. However, a power soft robot—defined as a robot driven by powerful soft actuators—has the potential to achieve the coexistence of high power and high compliance with a lightweight structure and a simple control method.

An approach to actuating a power soft robot is the McKibben artificial muscle due to its compliant structure [1] and its potential to generate high power with high pressure. A McKibben muscle consists of an inner inflatable rubber tube and outer braided cords. One of the simplest configurations of an adaptable compliant joint is to use two McKibben muscle actuators connected to the same joint in an antagonistic arrangement [2]. Most of the McKibben muscles obtain contraction force by injecting air into the inner chamber. However, such pneumatic artificial muscle (PAM) actuators have slow response time, low efficiency [3], and less generated power due to limited air pressure. Besides, they are not always safe enough but sometimes show dangerous behaviors due to air compressibility. For example, when a load weight acting on a robot is separated suddenly, or after a great

*Correspondence: feng.y.ac@m.titech.ac.jp
[1] Department of Mechanical Engineering, Tokyo Institute of Technology, 2-12-1 Okayama, Meguro-ku, Tokyo 152-8550, Japan
Full list of author information is available at the end of the article

disturbance is applied to the manipulator, stored pneumatic energy will be instantaneously released, and the manipulator driven by PAMs will rapidly oscillate. This uncontrollable oscillation, which is shown experimentally in the next section of this paper, greatly compromises the stability of robotic systems driven by PAMs. Therefore, PAM is not the optimal actuator for actuating a power soft robot.

Hydraulic artificial muscle actuators (HAM) with an incompressible liquid medium have better performance (including higher speed, accuracy, and power) due to their higher system stiffness and higher bandwidth compared with PAM [4–6]. In addition, due to the incompressibility of hydraulic fluid, a manipulator arm driven by HAMs does not rapidly oscillate when the load weight is suddenly released. With the advantages such as the high power of a hydraulic actuator and the compliant structure of an artificial muscle actuator, HAM is considered as a potential candidate for a power soft robot to achieve the coexistence of high power and high compliance in collaborative tasks.

Although a hydraulic muscle actuator is not compliant enough as a pneumatic muscle actuator, its better controllability makes it possible to give it higher compliance with active impedance control. The concept of impedance control was proposed by Hogan from an idea of human-like impedance control [7], which described dynamic behavior as a second-order mechanical system with the desired inertia, stiffness, and damping [8]. Impedance control focuses on the characterization and control of the interaction and effectively improves the dynamic compliance of the power soft robot driven by HAMs. However, little has been reported on the control of HAMs to improve the feasibility of human–robot interactions. Xiang et al. reported the combined hydraulic and pneumatic mode of McKibben muscle for interaction [9]. Slightam et al. reported the practicability of impedance control of a single hydraulic muscle [10].

Sufficient stability and dynamic compliance are the key factors to higher safety. With the impedance control proposed in this study, manipulator arm can be shifted by an operator or a disturbance with appropriate dynamic compliance, and the joint of the power soft robot driven by hydraulic muscles shows high stability in various scenarios. The high stability is characterized by no obvious oscillations and controllable reaction angular velocity against sudden load separation or cushioning ability against sudden impact disturbance.

The aim of this study is to show the potential of hydraulic muscles to realize safe power soft robots, which would be both powerful and soft. Next, we show the stability against sudden load change of a manipulator arm driven by hydraulic muscle actuators experimentally by comparing it with pneumatic actuators. In the subsequent section, we model the antagonistic joint and describe the characteristics of the joint. Further, a simple impedance control with the braking method is proposed to improve its dynamic compliance. Finally, performance, compliant motion, and disturbance reaction of the arm are shown experimentally to conclude that the robots driven by hydraulic muscles with the proposed control strategy have a great potential for implementing soft power robots.

Safety evaluation of artificial muscles for sudden load change

Characteristics of artificial muscles

In this study, we assume that the following conditions must be met to improve safety: (1) the robot should be compliant when subjected to an external force; (2) the robot should not oscillate when the external force or load changes suddenly; (3) the speed of movement is controllable, with no sudden peaks; (4) actuators cannot be seriously damaged and cannot cause the robotic arm to suddenly lose control in sudden situations; and (5) the robot needs to be light enough to reduce the harm to people in an inevitable conflict.

The actuating characteristics of actuators related to hydraulic muscles are compared in Table 1. Artificial muscles have the advantage of compliance, while hydraulic devices have the advantages of stability and power. The aramid fiber used in our artificial muscles has extremely high cutting resistance, so the artificial muscles with flexible structures also have relatively high puncture resistance. Even if the oil-resistant rubber is damaged, the burst risk is considerably small in hydraulic muscles as the oil pressure drops quickly after an oil leak. Because pneumatic muscles have decreased safety due to the compressibility of air and the resultant burst factor, hydraulic muscles are more robust and reliable actuators.

Pneumatic muscles and hydraulic muscles for experiments have an approximate length of 44 cm of an elastic inner bladder (shown in Fig. 1). The inner bladder is made of an oil-resistant nitrile rubber developed by Morita et al. [11] because hydraulic muscles require oil resistivity. The outer braided cords are made of aramid fiber. The weaving method and oil inlet adopt the same design used by Mori et al. [12]. They have the same outer radius of 0.8 cm. Figure 2 compares the different outer braid angles of a pneumatic muscle and a hydraulic muscle. The 25° braid angle of the pneumatic muscle has a greater contraction force-pressure ratio, so that a pneumatic muscle can produce the close contraction force at one-third internal pressure as that of the hydraulic muscle, without exceeding the air pressure resistance limit of one order of magnitude less. (See Fig. 3 and subsequent sections for

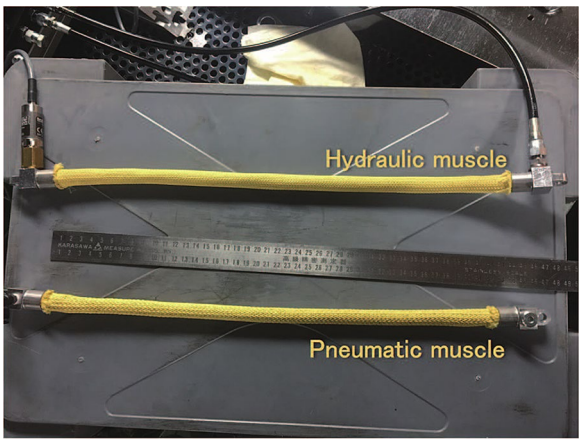

Fig. 1 Appearance of a hydraulic muscle and a pneumatic muscle. The two kinds of muscles have a similar appearance and the same natural length of 44 cm

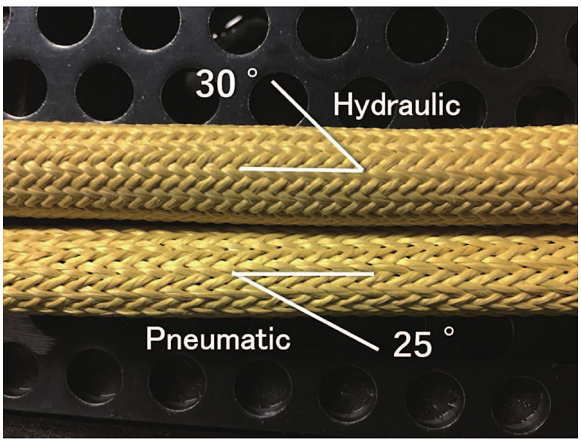

Fig. 3 Comparison of the contraction ratio and tension of a pneumatic muscle and a hydraulic muscle.Upper: contraction force of a pneumatic muscle. Bottom: contraction force of a hydraulic muscle

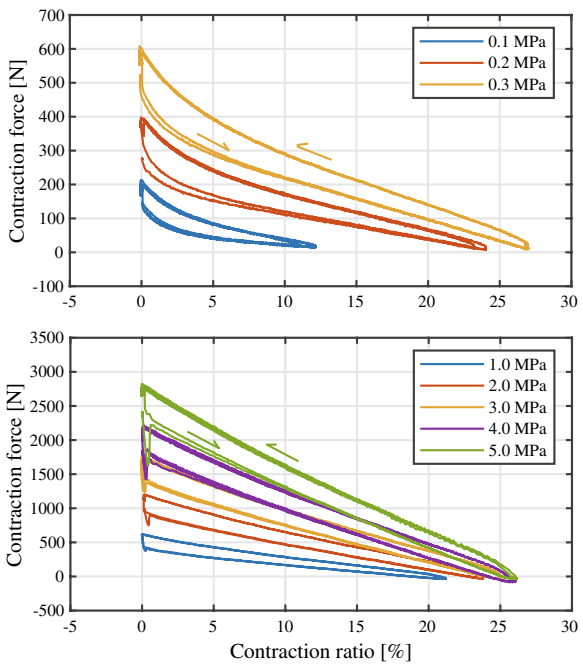

Fig. 2 Braid angle of a hydraulic muscle and a pneumatic muscle.

comparison experiments.) The 30° braid angle allows the hydraulic muscle to have a higher braided cord density to ensure that the rubber tube does not leak.

Compared with traditional robot actuators, artificial muscles are highly lightweight. In this study, a pneumatic muscle's weight is 112 g, and that of a hydraulic muscle is 124 g. Under the condition of maximum contraction, the maximum volume inside the hydraulic muscle is approximately 60 cm^3. When using oil with a density of 0.881 g/cm^3, the weight of oil present is approximately 52 g. Although the hydraulic muscles need to use extra hoses to provide oil supply, a robot driven by these muscles are more lightweight compare with driven by traditional hydraulic actuators (such as cylinders or hydraulic motors).

The characteristics of a single pneumatic muscle and a hydraulic muscle are shown in Fig. 3. Hydraulic muscles can generate much higher force than pneumatic muscles due to the higher available pressure (up to 7.0 MPa) applied to the muscle.

Safety evaluation experiment for sudden load separation

The stability of the pneumatic and hydraulic muscle driven manipulator against sudden load separation is one of the key safety factors and is therefore investigated in the sudden load separation experiment. In this case, the load is suddenly separated from the manipulator to observe its reaction, as stored elastic energy is suddenly released. Experiments are repeated in a one-side arrangement with a single muscle and an antagonistic arrangement with two muscles (both pneumatic and hydraulic). The experimental setup is shown in Fig. 4. The internal pressure is adjusted to a stable level in the beginning, and the supply circuit is blocked during the reaction. The workable rotational range of the joint is approximately ±28°, wherein the muscles are always straight and contracting in the axial direction.

In the sudden load separation experiment, the internal pressure of both hydraulic and pneumatic muscles is adjusted. A manipulator arm with a 10 kg weight load is at the horizontal position. Subsequently, the 10 kg load is separated, causing the arm to react. The reaction results of a single hydraulic and pneumatic muscle

Table 1 Comparison of actuators related to hydraulic muscles

Actuator	Backdrivability	Structural compliance	Stability under disturbance	Generating force	puncture resistance
Pneumatic cylinder	Relatively high	No	Relatively low	Low	High
Pneumatic muscle	High	High	Low	Low	Relatively high
Hydraulic cylinder	Low	No	High	High	High
Hydraulic muscle	Relatively high	Relatively high	Relatively high	High	Relatively high

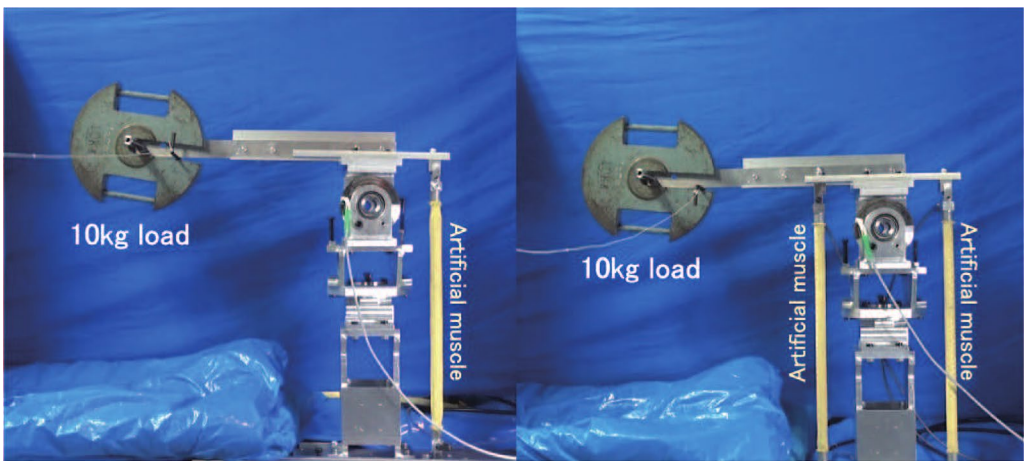

Fig. 4 Experimental setup for a sudden load change. Left: single arrangement. Right: the antagonistic arrangement with two muscles

connected to the joint are shown in Fig. 5, respectively. The initial pressure of a single pneumatic muscle is 0.4 MPa, but it is 1.0 MPa for a single hydraulic muscle due to the difference in the braid angles. For safety reasons, a stopper is installed at approximately 70° to avoid extreme reaction.

The reaction motion results of pneumatic and hydraulic muscles connected to the joint in an antagonistic arrangement are shown in Fig. 6, respectively. The initial internal pressure of the load-side pneumatic muscle is 0.1 MPa, whereas that of the other side is 0.4 MPa. The initial internal pressures of hydraulic muscles are 1.5 MPa and 2.5 MPa.

As shown in Fig. 5, the manipulator arm driven by a single pneumatic muscle has a considerable reaction to the angular displacement until being stopped by the stopper at 70°. Moreover, it oscillates with angular velocity max to 540°/*s* before hitting the stopper due to its high compliance and lack of damping. This high-speed oscillation has the potential to be extremely dangerous when an operator is present. In contrast, the system driven by a single hydraulic muscle reacts with a significantly lower peak value of angular velocity and displacement. The difference in angular velocity

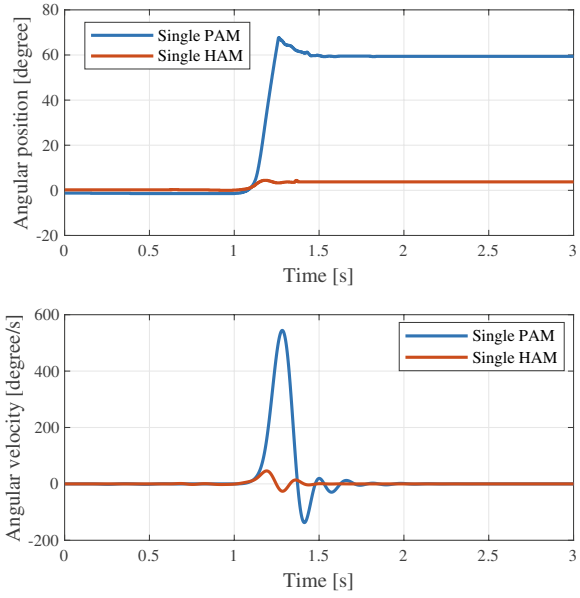

Fig. 5 Reactions of the joint driven by a single pneumatic muscle and hydraulic muscle when the 10 kg load is suddenly separated. The manipulator arm is stopped by the stopper at 70°

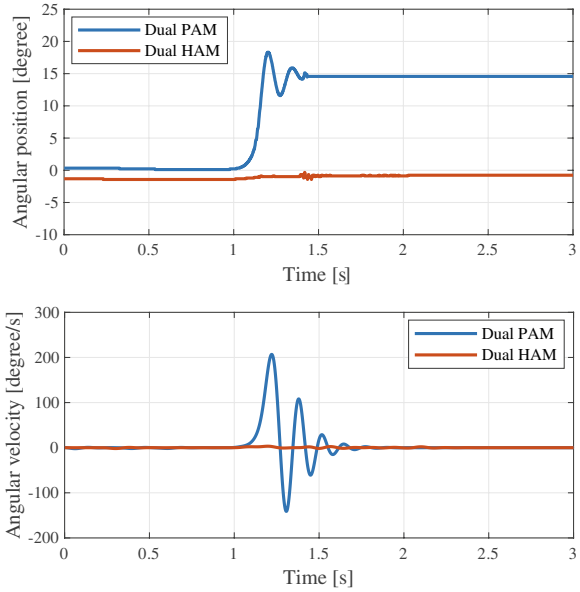

Fig. 6 Reactions of the antagonistic joint driven by pneumatic muscles and hydraulic muscles when the 10 kg weight is suddenly separated

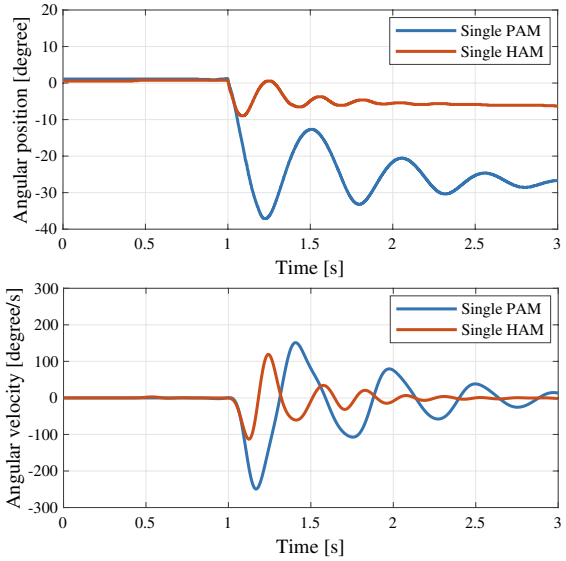

Fig. 7 Reactions of the joint driven by a single pneumatic muscle and hydraulic muscle impacted by a 10 kg load dropped from 8 cm height

indicates that the hydraulic muscle is more stable than the pneumatic muscle when the stored elastic energy is suddenly released.

When the joint is in the antagonistic arrangement driven by two artificial muscles (Fig. 6), both pneumatic and hydraulic muscles are more stable than when in a single arrangement. This can be explained as follows. In the antagonistic arrangement, torque depends on the differing contraction force of both sides. When one of the muscles is contracting, the muscle on the other side is elongating. Thus, the braid angle of the contracted muscle is increasing, and that of the elongated one is decreasing. The internal volume also changes. The contracted muscle has a lower pressure with a higher braid angle to generate lower force, and the elongated muscle generates higher pressure with a lower braid angle to generate higher force. With the same angular displacement, the antagonistic arrangement generates higher torque compared with that of the single arrangement. However, uncontrollable oscillation due to air compressibility still exists, which can possibly injure the operator during movement. Instead, the hydraulic muscle can provide a smoother reaction as stored elastic energy is released, especially in the antagonist arrangement wherein the peak of reaction angular velocity is at a considerably low level, and no oscillation occurs due to its high stiffness, making the hydraulic muscle suitable to drive a power soft robot.

Safety evaluation experiment for sudden impact disturbance

The stability and appropriate compliance of the manipulator driven by pneumatic and hydraulic muscles against sudden impact disturbance is another safety key factor and is therefore investigated in the sudden impact disturbance experiment. Similar to the sudden load separation experiment, the manipulator is adjusted to the horizontal position with stable internal pressure and the supply circuit is blocked during the reaction. We then drop a 10 kg weight load from a height of about 8 cm as a sudden impact disturbance input.

The reaction results of a single hydraulic and pneumatic muscle connected to the joint are shown in Fig. 7. The initial pressures of the single pneumatic muscle and the single hydraulic muscle are 0.1 MPa and 0.4 MPa, respectively.

The reaction motion results of pneumatic and hydraulic muscles connected to the joint in an antagonistic arrangement are shown in Fig. 8. The initial internal pressures of both pneumatic muscles are 0.25 MPa, and the initial internal pressures of both hydraulic muscles are 2.0 MPa.

It can be seen from Fig. 7 that after being impacted by a falling 10 kg weight load at 1.0 s, both single muscles show strong oscillation. Similar to the sudden load separation result, a single pneumatic muscle shows a greater displacement and longer oscillation due to the lack of damping and high compliance. The maximum

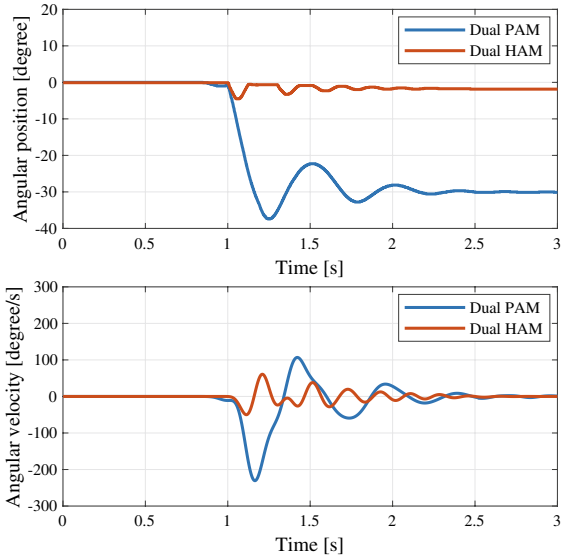

Fig. 8 Reactions of the antagonistic joint driven by pneumatic muscles and hydraulic muscles impacted by a 10 kg load dropped from 8 cm height

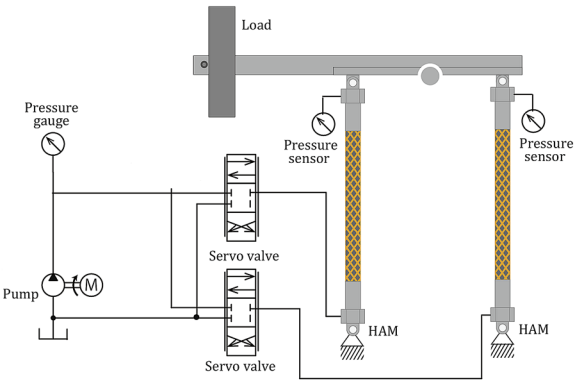

Fig. 9 Schematic diagram of the antagonistic joint. Consists of a rotary encoder, two servovalves, two hydraulic muscles, and their pressure sensors

angular velocity has reached approximately twice that of a single hydraulic muscle, reaching approximately $250°/s$.

In the antagonistic arrangement, the maximum displacement and the maximum angular velocity of the hydraulic muscle decrease significantly. When returning back to the horizontal position, the hydraulic muscle stops close to the horizontal position due to the contraction force of the load-side muscle and then oscillates due to the impact of the bounced load. In contrast, although there is a reduced oscillation time of the pneumatic muscles with antagonistic arrangement, the maximum angular velocity is relatively close to that of a single muscle. The maximum angular velocity still reached close to approximately $230°/s$, which compromises the stability of the manipulator arm due to air compressibility.

However, neither the hydraulic muscles nor the pneumatic muscles showed sufficient safety in the sudden impact disturbance experiment. The excessive angular velocity of the pneumatic muscle in both arrangements may easily cause the operator to be injured. The hydraulic muscles show higher stability in a particularly antagonistic arrangement. However, due to lack of sufficient compliance, falling heavy objects may bounce up and injury the operator. Therefore, we consider an effective way to improve the safety of the antagonistic joint driven by hydraulic muscles by improving its dynamic compliance with an active control method without losing its stability.

Modeling the antagonistic joint

According to Schulte [13] and Chou [14], the contraction force F_i of a McKibben artificial muscle can be expressed by Eq. (1) with internal pressure P_i, where φ is the braid angle; b, n are the length of an aramid fiber and number of turns, respectively. Index i represents the number of the artificial muscle.

$$F_i = \frac{\pi P_i}{4}\left(\frac{b}{n\pi}\right)^2 (3\cos^2\varphi - 1) \tag{1}$$

As depicted in Eq. (1), contraction force decreases with an increase in the braid angle. Using geometric calculation, the relationship between contraction ratio and force is calculated to be close to a straight line for a hydraulic muscle with a larger initial braid angle, which is also in line with the measured results shown in Fig. 3. Therefore, to simplify the modeling and make the relationship between the contraction ratio and force more intuitive, we use a simple linear expression to model the contraction force of the hydraulic muscle, as in Eq. (2):

$$F_i = K_f P_i(\epsilon_{\max} - \epsilon_i), \tag{2}$$

where P_i is the internal pressure; ϵ_i and $\epsilon_{\max}$ are the contraction ratio and maximum contraction ratio, respectively. The proportionality constant K_f depends on the initial outer diameter and the initial braid angle of the artificial muscle. For the hydraulic muscle, the maximum contraction ratio $\epsilon_{\max}$ is considered to be 26% from Fig. 3.

The schematic diagram of the antagonistic joint is shown in Fig. 9. The hydraulic muscle on the load-side and the hydraulic muscle on another side have indices 1 and 2, respectively. Generated torque τ_{sum} is given by Eq. (3). Moreover, r is the distance between the muscles and the center of rotation.

$$\tau_{\text{sum}} = F_2 r - F_1 r \tag{3}$$

Passive compliance of the antagonistic joint

Ignoring the self-weight, when there is no torque received and no torque generated, $\tau_{\text{sum}} = 0$. Internal pressures of hydraulic muscles 01 and 02 are $P_1 = P_{\text{avg}} - \Delta P_{\text{pos}}$ and $P_2 = P_{\text{avg}} + \Delta P_{\text{pos}}$, respectively. Moreover, ΔP_{pos} is the pressure difference from the average pressure, which ensures that the manipulator arm stays in a certain position without generating the torque shown in Eq. (4). Finally, ϵ_{hor} is the contraction ratio of the two hydraulic muscles when the manipulator arm is at the horizontal position, θ represents the angular position, and L represents the natural length of the muscle (44 cm).

$$\Delta P_{\text{pos}} = P_{\text{avg}} \frac{\theta r}{L(\epsilon_{\text{max}} - \epsilon_{\text{hor}})} \tag{4}$$

When external torque τ_{ext} and gravitational torque τ_{sel} of self-weight are received (shown in Fig. 10), the passive torque τ_{pass} generated by the antagonistic joint is shown in Eq. (5), where $\Delta\theta_{\text{dis}}$ represents the angular displacement caused by both external torque and self-weight. The internal volume change of the muscles will cause internal pressure changes. However, angular displacement and internal volume deformations are assumed to be minimal. For this reason, the internal pressure is assumed to be the same as when no torque is received.

$$\begin{aligned}\tau_{\text{pass}} &= \frac{K_{\text{f}}(\theta + \Delta\theta_{\text{dis}})r^2}{L}(2P_{\text{avg}}) \\ &\quad + K_{\text{f}}(\epsilon_{\text{max}} - \epsilon_{\text{hor}})r(2\Delta P_{\text{pos}}) \\ &= \frac{2P_{\text{avg}}K_{\text{f}}r^2}{L}\Delta\theta_{\text{dis}}\end{aligned} \tag{5}$$

Notably, although the contraction ratios and the internal pressure of the two muscles are not the same when the initial position of the robot arm is at any angular position other than $\theta = 0$, passive torque generated from angular displacement with constant internal pressure is a constant value. Compliance is inversely proportional to the average internal pressure. By adjusting the average pressure, the passive impedance characteristic of the joint can be adjusted, which is also similar to the human muscles. Therefore, the joint can be regarded as a soft joint with fixed compliance in any angular position with a certain average internal pressure.

Fluid resistance of the hydraulic muscle

The hydraulic pressure dynamic in one of the muscles is modeled via hydraulic flow through a variable cross-sectional orifice in a plate and the rate of change in the internal volume of the muscle. According to Fig. 9, each servovalve is considered to be a linear-variable cross-sectional orifice in a plate. Subsequently, the relationship among the internal pressure dynamic $\dot{P}_i$, the internal volume dynamic $\dot{V}_i$ of the rubber tube, and the flow rate Q_i of oil in and out of the rubber tube is expressed by Eq. (6), where β is the bulk modulus of the hydraulic oil.

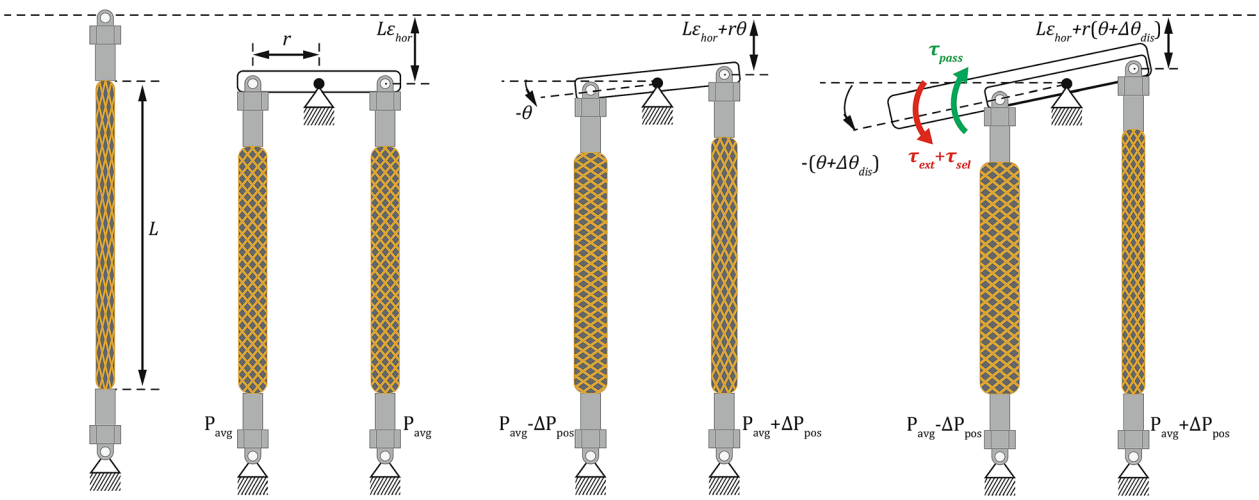

Fig. 10 Passive compliance of the antagonistic joint. (1) Nature length of a hydraulic muscle. (2) Horizontal position with the same internal pressure P_{avg}. (3) Certain initial position with different internal pressures. (4) Passive torque τ_{pass} generated from angular displacement $\Delta\theta_{\text{dis}}$ caused by external torque τ_{ext} and gravitational torque τ_{sel} received

$$\dot{P}_i = \frac{\beta}{V_i}(Q_i - \dot{V}_i) \tag{6}$$

The ideal flow rate Q_i is expressed in Eq. (7), where K_{val} is the opening ratio of the servovalve, which depends on the command voltage; A is the maximum opening area, C_d is the discharge coefficient, and ρ is the density of the hydraulic oil. Moreover, P_i is the internal pressure; P_{src} and P_{atm} are the source pressure and the atmospheric pressure, respectively.

$$Q_i = \begin{cases} K_{\text{val}} A C_d \sqrt{\frac{P_{\text{src}} - P_i}{\rho}} & 0 < K_{\text{val}} < 1 \\ 0 & K_{\text{val}} = 0 \\ K_{\text{val}} A C_d \sqrt{\frac{P_i - P_{\text{atm}}}{\rho}} & -1 < K_{\text{val}} < 0 \end{cases} \tag{7}$$

From Eqs. (6) and (7), when an ideal pressure source that can maintain the specified pressure is used, the change in internal pressure is determined by the opening size of the servovalve and the change in volume. The internal volume of the rubber tube is mainly determined by the contraction ratio of the hydraulic muscle. However, it also slightly changes when the muscle radial expands due to a change of internal pressure. This feature of slightly variable volume makes a hydraulic artificial muscle different from a hydraulic cylinder. In addition, the volume change is opposite to the hydraulic cylinder: the volume becomes smaller when elongated.

For an antagonistic joint, the muscle on one side is contracting, and the muscle on the other side is forced to elongate, while the rotation of the joint is subjected to a large external torque. The internal volume of the elongated muscle will be quickly compressed, and if the valve opening size allows the oil out of the muscle at a low level (which means that the theoretical outflow rate is not large enough), the compression of internal volume will raise the internal pressure. Subsequently, the hydraulic oil is forced to pass through the servovalve, and then it flows into the oil tank. This fluid resistance then acts as a damping force. This feature can be used to adjust the damping, which would be impossible with pneumatic muscles.

Dynamic model of the antagonistic joint

With additional actuation pressure difference ΔP_{act}, the actuation torque generated (shown in Fig. 11) at a certain angular position θ is shown in Eq. (8). Internal pressures of hydraulic muscles 01 and 02 are $P_1 = P_{\text{avg}} - \Delta P_{\text{pos}} - \Delta P_{\text{act}}$ and $P_2 = P_{\text{avg}} + \Delta P_{\text{pos}} + \Delta P_{\text{act}}$, respectively.

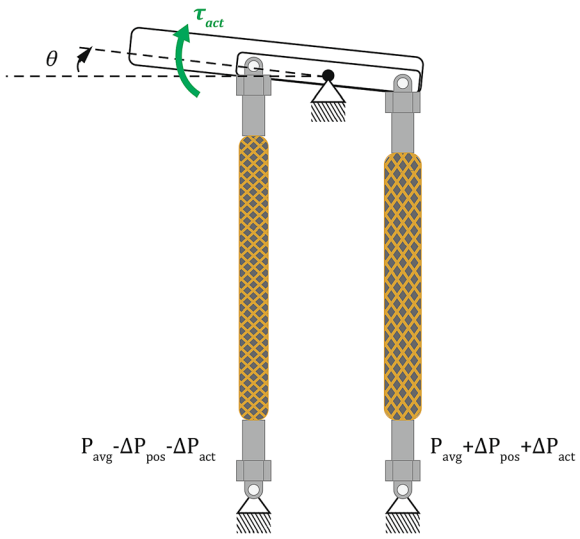

Fig. 11 Actuation torque by pressure difference at a certain angular position. Pressure difference ΔP_{pos} for certain angular position θ is shown in Eq. (4). Relationship between ΔP_{act} and actuation torque τ_{act} is shown in Eq. (8)

$$\begin{aligned} &\tau_{\text{act}} \\ &= K_{\text{f}}(P_{\text{avg}} + \Delta P_{\text{pos}} + \Delta P_{\text{act}})(\epsilon_{\max} - \epsilon_{\text{hor}} - \frac{\theta r}{L})r \\ &\quad - K_{\text{f}}(P_{\text{avg}} - \Delta P_{\text{pos}} - \Delta P_{\text{act}})(\epsilon_{\max} - \epsilon_{\text{hor}} + \frac{\theta r}{L})r \\ &= 2K_{\text{f}}(\epsilon_{\max} - \epsilon_{\text{hor}})\Delta P_{\text{act}} r \end{aligned} \tag{8}$$

By analogy with the passive torque from angular displacement shown in Eq. (5), actuation torque is proportional to the actuation pressure difference at any angular position.

Safety-enhanced control strategy of the antagonistic joint

Compliance and low inertia are the two basic characteristics of safe robotic systems [15]. To improve its dynamic impedance characteristics, we propose a simple impedance control strategy to utilize the features of the hydraulic muscle.

In this study, by taking advantage of the compliant structure and incompressible liquid medium of a hydraulic muscle, we proposed a simple second-order impedance control to improve the dynamic characteristics of the antagonist joint. When located near the desired angular position, the manipulator arm is braked by closing both servovalves. Moreover, when the manipulator leaves the commanded position for more than a certain range, impedance control adjusts the internal pressure of both muscles. Comparison of the proposed control and

Table 2 Comparison of controllers

Controller	Controlled variable	Accuracy	Dynamic compliance	Stability
Position PID	Position	High	No	High
Compliance control	Internal pressure	Relatively low	Adjustable compliance	Relatively high
Impedance control	Internal pressure	Relatively low	Adjustable compliance, damping and inertia	Low
Proposed control	internal pressure	low	adjustable compliance, damping and inertia	relatively high

other ordinary strategies is shown in Table 2. The braking method enhances the stability of impedance control by eliminating the over-shoot during low-damping impedance control when the manipulator arm approaching to the desired position.

Impedance control comprises an outer impedance loop and an inner loop. The control block diagram is shown in Fig. 12. Model-based feedback corrects the contraction force when the braid angle is changed. The outer loop outputs the desired internal pressure of each muscle to the inner loop based on the dynamic state measured by the encoder. The pressure control of the two muscles in their inner loop is a simple proportional control, and the desired pressure is tracked by adjusting the opening size of the servovalves in both hydraulic circuits. For better realization of human–robot interaction, the impedance controller is set to guarantee high apparent compliance.

The desired internal pressure of both muscles is shown in Eq. (9), where P_{d1} and P_{d2} are the desired pressures of the load-side muscle and the opposite muscle, respectively. In addition, P_{avg} is the average internal pressure. Model-based feedback ΔP_{pos} and self-weight compensation ΔP_{sel} represent the pressure differences required to ensure that the manipulator can stay at the desired angular position, respectively. Moreover, ΔP_{act} represents the actuation pressure difference, which generates actuation torque to the joint to improve its apparent impedance, including apparent stiffness, damping, and inertia.

$$\begin{aligned} P_{\mathrm{d1}} &= P_{\mathrm{avg}} - \Delta P_{\mathrm{pos}} - \Delta P_{\mathrm{sel}} - \Delta P_{\mathrm{act}} \\ P_{\mathrm{d2}} &= P_{\mathrm{avg}} + \Delta P_{\mathrm{pos}} + \Delta P_{\mathrm{sel}} + \Delta P_{\mathrm{act}} \end{aligned} \tag{9}$$

Concept of impedance control with the braking method

When an external force is received at the initial position, the compliant structure of the artificial muscles allows the manipulator arm to be rotated in a small angular displacement, although the servovalves are closed. After this angular displacement, a second-order impedance control was used to adjust the actuation torque to decrease the apparent stiffness, damping, and inertia. Because of the existence of the second-order term, the actuation torque will change shortly when the external force changes during the movement. Subsequently, when the external force disappears, and the manipulator arm returns to its initial position, the arm rotates quickly under the second-order impedance control. When it is approaching the initial position in the braking range, both servovalves will be closed quickly. Under the friction of the artificial muscles themselves and the increased fluid resistance, the manipulator arm will brake and stabilize near the initial commanded position. This control strategy also helps

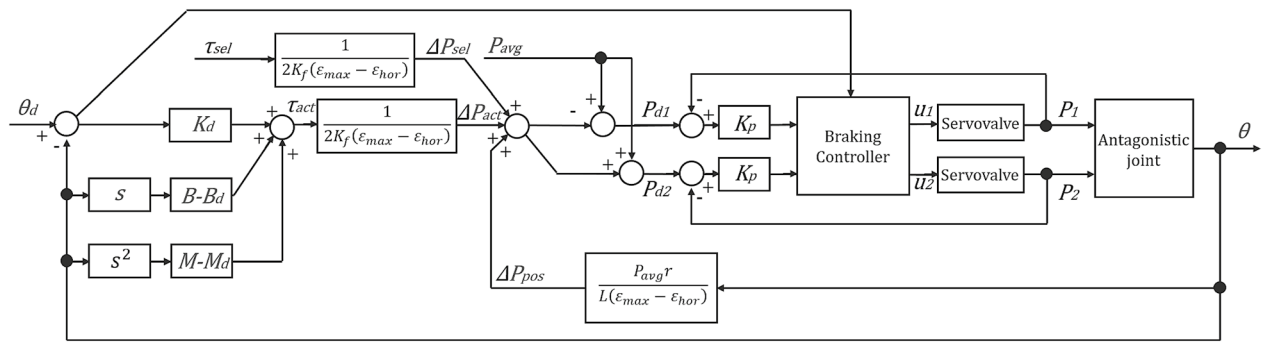

Fig. 12 Block diagram of the variable second-order impedance control. The outer loop outputs the internal pressure difference equals $\Delta P_{\mathrm{act}} + \Delta P_{\mathrm{pos}} + \Delta P_{\mathrm{sel}}$, and the desired internal pressure of both muscles is shown in Eq. (9). Each inner loop includes a braking controller; which controls whether the servovalve is closed or not; the control law is shown in Eq. (13)

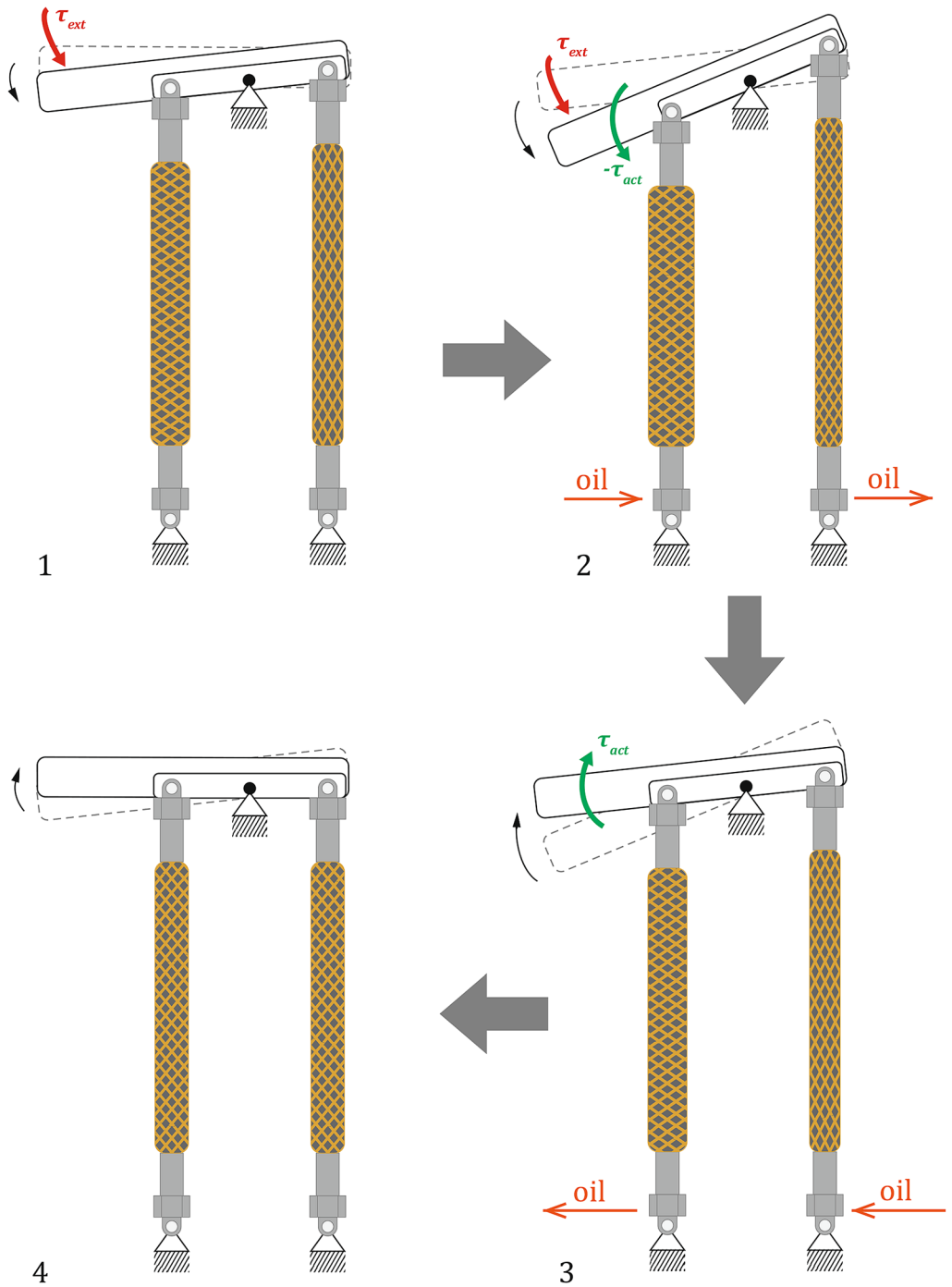

Fig. 13 Reaction phases of the antagonistic joint when external torque from the operator is received. (1) Small displacement with a compliant structure of the hydraulic muscle. (2) Second-order impedance control is fully involved to reduce the apparent inertia and damping. (3) When the external torque disappears, angular velocity is increased to overcome the hysteresis nonlinearity of the muscle when returning. (4) It brakes and stabilizes near the initial position with blocked servovalves

reduce the lack of driving torque and the angular position errors caused by the hysteresis of the contraction force generated by both artificial muscles during returning to the initial angular position. The whole reaction process—when receiving the external force—is shown in Fig. 13.

This simple safety-enhanced impedance control strategy uses the compliant structure of the artificial muscle and the characteristics of the fluid medium, which is a control strategy that can only be achieved by hydraulic artificial muscles. A pneumatic muscle cannot use fluid characteristics to control speed or adjust the damping. A hydraulic cylinder or hydraulic motor cannot quickly deform if a valve is blocked when the external force is received. Because the initial displacement utilizes structural compliance, this impedance control strategy can be realized by a low-frequency controller, which is not possible with traditional motor-driven mechanisms. Moreover, series elastic actuator increases complexity and weight.

Model-based feedback and self-weight compensation

As mentioned, if one muscle contracts, the other muscle must elongates. The change in their braid angle will cause the contracted muscle to produce less force under the same internal pressure, while the elongated one will generate more contraction force. Therefore, a simplified linear model is applied as feedback to correct the desired pressure in both muscles. Internal pressure differences ΔP_{pos} and ΔP_{sel} of the two muscles when the manipulator stays at a certain commanded angular position are shown in Eq. (10). Here, ΔP_{pos} is consistent with Eq. (4): the internal pressure difference required for the robot arm to maintain a certain angular position. Moreover, ΔP_{sel} is used to compensate for the gravitational torque from self-weight. As a one-degree-of-freedom joint with a limited range of rotation, the gravitational torque from the self-weight is assumed to be a fixed value.

$$\begin{aligned} \Delta P_{\mathrm{pos}} &= P_{\mathrm{avg}} \frac{r}{L(\epsilon_{\max} - \epsilon_{\mathrm{hor}})} \theta \\ \Delta P_{\mathrm{sel}} &= \frac{\tau_{\mathrm{sel}}}{2K_{\mathrm{f}}(\epsilon_{\max} - \epsilon_{\mathrm{hor}})r} \end{aligned} \tag{10}$$

Under the correction of this model-based feedback and self-weight compensation, the manipulator arm can stay at any commanded angular position, and the minimum stiffness can be set to zero within the rotation range.

Second-order impedance controller

In this study, we focus on how impedance control can adjust the apparent impedance of the antagonistic joint to enhance its safety rather than precise control to implement target dynamics. Therefore, we ignore the dynamic characteristics (fluid resistance, compliance) and use a simple variable impedance controller.

Assuming that the manipulator arm is a simple rigid joint with only frictional damping, its simplified dynamic model and the desired second-order behavior are shown in Eq. (11), where τ_{ext} is the external torque received; B, M are the frictional damping and inertia of the manipulator; $K_{\mathrm{d}}, B_{\mathrm{d}}, M_{\mathrm{d}}$ are the desired virtual stiffness, damping, and inertia, respectively.

$$\begin{aligned} M\ddot{\theta} + B\dot{\theta} + \tau_{\mathrm{ext}} &= \tau_{\mathrm{act}} \\ K_{\mathrm{d}}(\theta_{\mathrm{d}} - \theta) + B_{\mathrm{d}}(\dot{\theta}_{\mathrm{d}} - \dot{\theta}) + M_{\mathrm{d}}(\ddot{\theta}_{\mathrm{d}} - \ddot{\theta}) &= \tau_{\mathrm{ext}} \end{aligned} \tag{11}$$

From Eq. (11), assuming that the desired angular velocity and the desired angular acceleration are zero, a simple variable impedance controller can be obtained, shown in Eq. (12) in the form of actuation pressure difference.

$$\Delta P_{\mathrm{act}} = \frac{K_{\mathrm{d}}(\theta_{\mathrm{d}} - \theta) + (B - B_{\mathrm{d}})\dot{\theta} + (M - M_{\mathrm{d}})\ddot{\theta}}{2K_{\mathrm{f}}(\epsilon_{\max} - \epsilon_{\mathrm{hor}})r} \tag{12}$$

Combining Eqs. (9), (10), and (12), the control laws of two servovalves are shown in Eq. (13), respectively.

$$\begin{aligned} u_1 &= \begin{cases} K_{\mathrm{p}}\left(P_{\mathrm{avg}} - \Delta P_{\mathrm{pos}} - \Delta P_{\mathrm{sel}} - \Delta P_{\mathrm{act}} - P_1\right) & \text{if } |\theta - \theta_{\mathrm{d}}| \geq R \\ 0 & \text{if } |\theta - \theta_{\mathrm{d}}| < R \end{cases} \\ u_2 &= \begin{cases} K_{\mathrm{p}}\left(P_{\mathrm{avg}} + \Delta P_{\mathrm{pos}} + \Delta P_{\mathrm{sel}} + \Delta P_{\mathrm{act}} - P_2\right) & \text{if } |\theta - \theta_{\mathrm{d}}| \geq R \\ 0 & \text{if } |\theta - \theta_{\mathrm{d}}| < R \end{cases} \end{aligned} \tag{13}$$

Here, u_1, u_2 are the commanded opening ratios; K_{p} is the proportional gain; ΔP_{pos} and ΔP_{sel} are the pressure difference for model-based feedback and self-weight compensation term shown in Eq. (10), respectively; ΔP_{act} is the actuation pressure difference to adjust apparent impedance shown in Eq. (12); R is defined as a braking range discussed in the concept of impedance control in the braking method section, which is the angular range of setting the servovalves to be closed. A higher braking range setting means that when receiving an external force, the manipulator arm needs to passively rotate a larger range with the blocked servovalves before the impedance control is involved; this results in a large initial apparent stiffness that is not easy to be moved at the beginning. However, a smaller braking range will close the servovalves too late when returning to the initial position, and the manipulator arm cannot be braked well. Considering the strength of the operator and the average hydraulic pressure of the muscles, the braking range R is

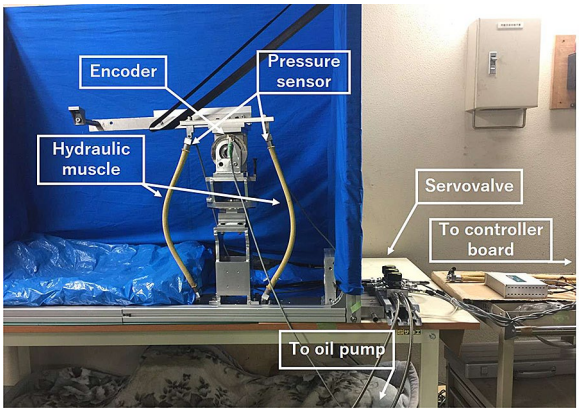

Fig. 14 Experimental setup for antagonistic joint driven by hydraulic muscles with impedance control

experimentally set as a range of ±1° above and below the desired angular position.

Experimental results and discussion

The experimental setup is shown in Fig. 14. Two hydraulic pressure sensors and a rotary encoder are used to monitor the internal pressure of two muscles and the motion of the manipulator arm. Two servovalves are controlled via dSPACE DS1104 using Simulink environment. The block diagram of impedance contorl is shown in Fig. 12 and experimental conditions are shown in Table 3.

Compliance and stability experiments of impedance control with baking method

Compliant reaction experiment

For the compliant reaction experiment, the manipulator arm starts at the horizontal position. A 5 kg load was used to emulate the external force generated by the operator during human–robot interaction. The initial angular position is set to 0°, the average internal pressure is set to 1.5 MPa, and the supply pressure is set to 3.0 MPa. The compliant reaction comparison when the 5 kg load was appended at 1.0 s is shown in Fig. 15. The commanded opening ratio is proportional to the command voltages applied to servovalves.

From Fig. 15, without active impedance control, servovalves are closed all the time. Therefore, the apparent stiffness was high when the external force was received. As a comparison, impedance control responded with a compliant reaction. The 1° displacement and pressure change in the first 0.6 s just after receiving the external force was caused by the deformation of hydraulic muscles while the servovalves were closed in the braking range. The internal pressure of the load-side muscle and the opposite-side muscle are decreasing and increasing due to the change of the internal volume, respectively. Starting from 1.6 s, angular displacement exceeds the ±1° braking range, and impedance control adjusts the internal pressure of two muscles. The average pressure quickly decreases to the set value. Subsequently, the two muscles begin to actively pressurize and decompress to improve their dynamic compliance. Finally, the system is stabilized at approximately 24° due to the low stiffness setting

When the hydraulic muscle antagonistic joint receives external force under impedance control, it first produces a displacement through the deformation of the muscle themselves and then the impedance control becomes involved to enhance the dynamic compliance of the joint. The passive compliance before involving control can also be adjusted by changing the braking range and average pressure. The controller does not need to operate continuously at a high frequency as this control method uses its own compliant structure, making it different from the hydraulic cylinder. As a result, the several-kilogram-level external force generated by an operator can easily shift the antagonistic manipulator arm driven by hydraulic muscles with the proposed impedance control, wherein its dynamic compliance is improved for safer human–robot interaction.

Sudden load separation experiment

The sudden load separation reaction comparison is the same as in the above section by separating a 10 kg weight load. The initial angular position is set at 0°, with the 10 kg load attached. The manipulator is stabilized at approximately −32° with impedance control and passively displace to −1.6° without impedance control. The reaction after the 10 kg load is suddenly separated at 1.0 s is shown in Fig. 16.

Impedance control with the braking method responded with a smooth reaction until the initial commanded position. When the manipulator arm reaches

Table 3 Default experimental conditions of impedance control

Control cycle	1 ms	Supply pressure	3.0 MPa
Braking range	±1°	Average pressure	1.5 MPa
Virtual stiffness K_d	0.02 MPa/ deg	Damping compensation $B - B_d$	0.02 MPa · s/deg
Proportional gain K_p	50 $\%_{opening}$/MPa	Inertia compensation $M - M_d$	0.0005 MPa · s^2/deg

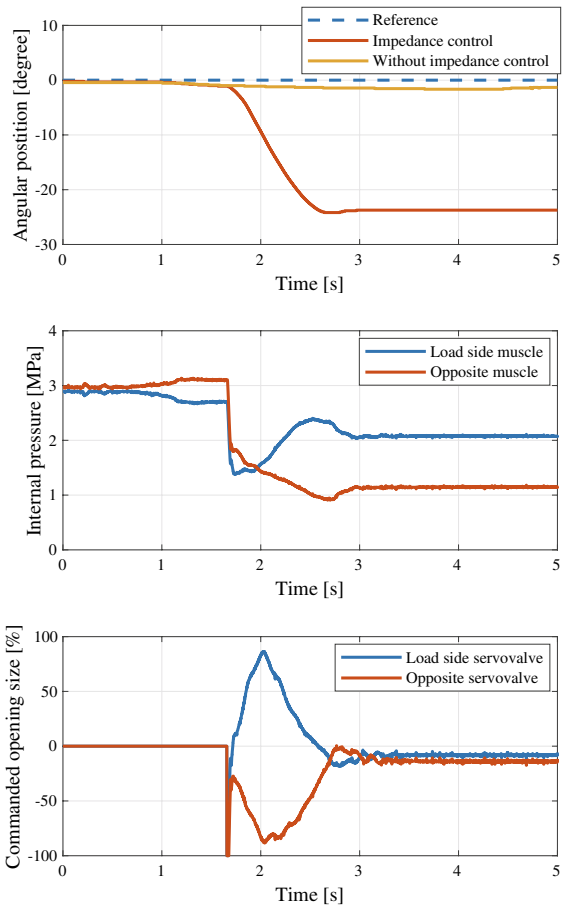

Fig. 15 Compliance comparison when the 5 kg load is attached. Upper: comparison of the angular position change. Middle: the internal pressure change of two muscles with impedance control. Bottom: the commanded opening size of two servovalves, where 0% is considered as fully closed. Positive means pressurization, and negative means decompression

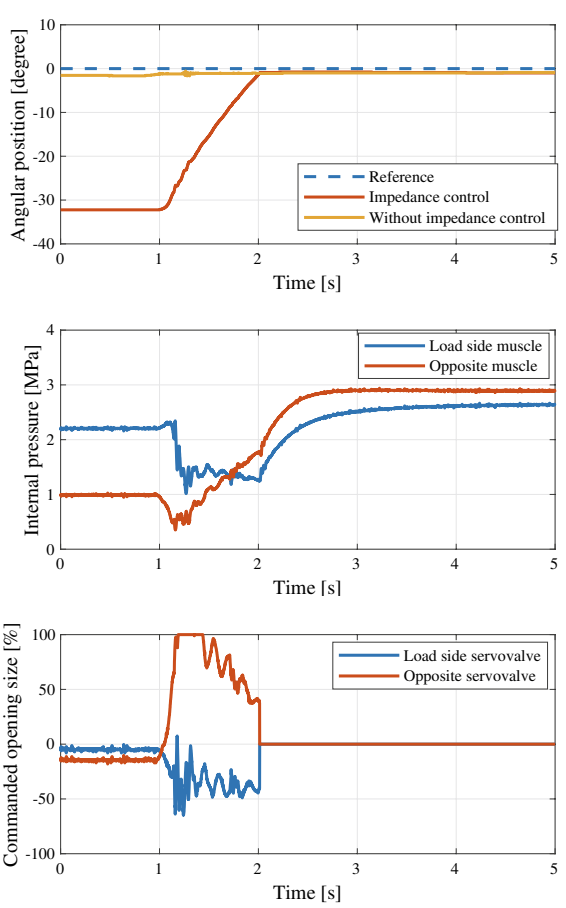

Fig. 16 Reaction comparison when the 10 kg load is suddenly separated. Upper: comparison of the angular position change. Middle: the internal pressure change of two muscles with impedance control. Bottom: the commanded opening size of two servovalves

the braking range ±1° at 2.0 s, both servovalves are quickly commanded to be closed. Under the damping effect of the hydraulic muscles, the manipulator arm is quickly braked and stabilized near the initial position. It is considered to be much safer than the pneumatic muscles because the peak value of response angular velocity is limited by the flowrate of servovalves. Moreover, no significant overshoot or oscillation appears compared with the pneumatic muscles.

Notably, when the impedance control is no longer involved, and both servovalves remain blocked starting at 2.0 s, the internal pressure of two muscles is increasing and is finally stopped at a much higher value than the desired average internal pressure of 1.5 MPa but closer to the supply pressure of 3.0 MPa. This can be considered as the result of the oil leakage of zero-lapped spool servovalves.

As a result, unlike pneumatic muscles, the manipulator arm driven by hydraulic muscles with impedance control simply returns to its initial position with controllable speed after the load weight is suddenly separated or after a great impact.

Performance experiments

Step response experiment

The step response is shown in Fig. 17. The manipulator arm is commanded to rotate between −15° and 15°.

At 1.0 s, impedance control starts to adjust the internal pressure to rotate the manipulator arm. When the manipulator arm reaches 14° at 2.2 s, it reaches the braking range. The servovalves are closed, and the arm is quickly braked. Due to the larger angular position of

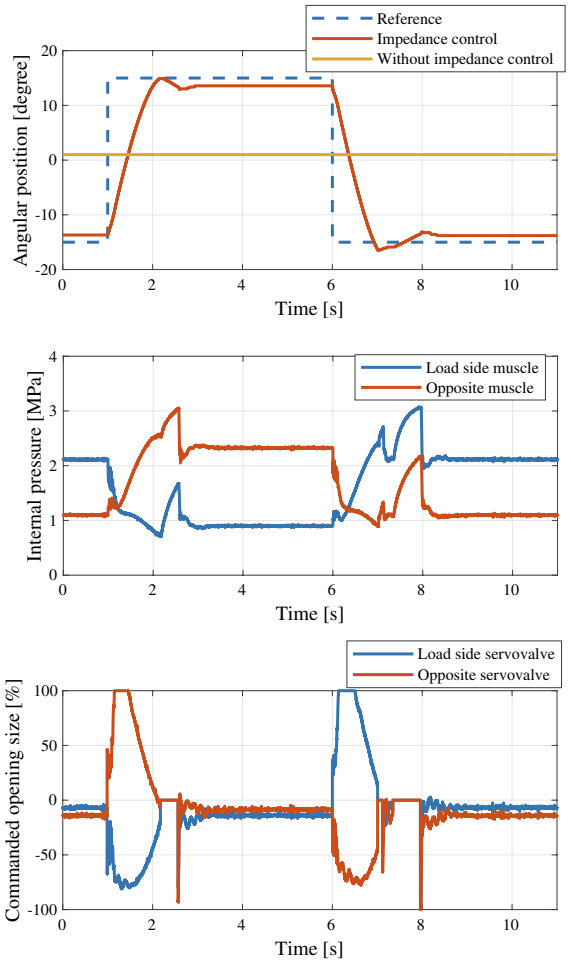

Fig. 17 Step response of the impedance control. Upper: comparison of the angular position change. Middle: the internal pressure change of two muscles with impedance control. Bottom: the commanded opening size of two servovalves. Manipulator arm rotates between −15° and 15°

the arm, the internal pressures of the muscles on the two sides are significantly different. The increase in pressure caused by the oil leakage in the servovalves is also different. In the interval from 2.2 to 2.6 s, the internal pressure of the elongated muscle rises higher than the other one. Hence, a reverse torque is generated, which leads the manipulator arm to leave the braking range. Although closing the valve can effectively brake the manipulator arm, oil leakage will cause the manipulator arm to hardly stay in the ±1° braking range when its angular position is much larger or smaller than the horizontal position, resulting in lower accuracy.

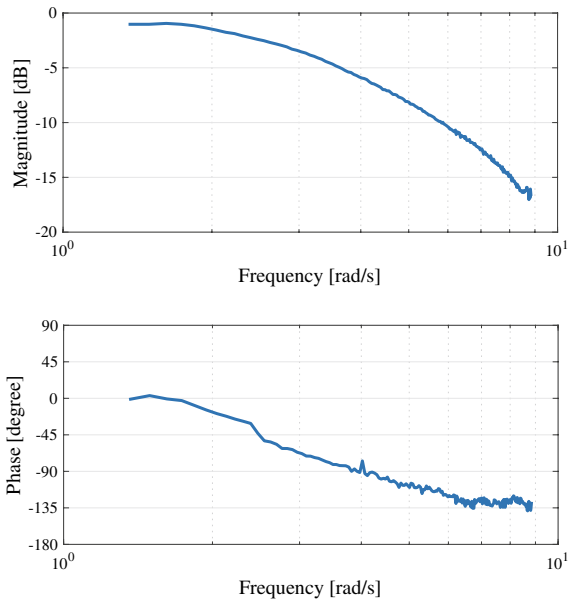

Fig. 18 Bode plots of the impedance control. Chirp input with amplitude of 20°

Bode plot

We applied a chirp input to draw the Bode plots which amplitude is set as 20°. The Bode plots are shown in Fig. 18

Referring to Figs. 16 and 17, the braking method will slow the manipulator arm when it is close to the desired position so that there will be no large overshoot under a low damping setting. This makes the system have a larger phase margin and better stability than ordinary impedance control under the same impedance setting.

Compared with common hydraulic actuators, the response speed of an antagonistic joint is lower. The main reason for the low speed is that the operating pressure of hydraulic muscles is much lower. In order to ensure that the hydraulic pressure does not exceed the pressure resistance of the hydraulic muscle, the supply pressure is set at 3.0 MPa. For the general servovalves used, this pressure is lower than the corresponding supply of 21 MPa, which results in a flowrate that is much lower compared to the hydraulic cylinder.

Adaptability to sudden impact disturbance

Impedance control can adjust impedance parameters to improve safety according to the situation. For example, adopting a higher dynamic compliance setting when directly collaborating with an operator, or reducing compliance to enhance stability in situations such as disaster relief.

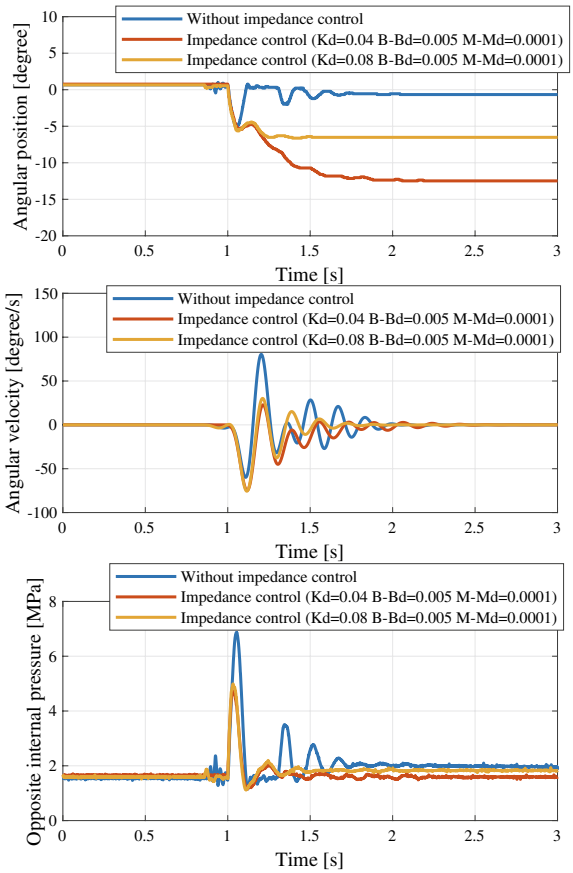

Fig. 19 Reaction comparison impacted by a 10 kg load dropped by 15 cm. Upper: comparison of the angular position change with different impedance parameter settings. Middle: comparison of the angular position velocity. Bottom: comparison of the internal pressure of the muscle on the opposite side of the load

Here, we reduced the apparent compliance and increased the damping and inertia to improve the stability under sudden impact disturbance, while the rest of the experimental conditions remain unchanged.

Similar to the safety evaluation section, we also used the dropped load to evaluate the improvement of the safety of the antagonistic joint under the impedance control. We used a 10 kg load with greater impact to drop from 15 cm. The reaction results are shown in Fig. 19, which includes the pressure change of the muscle on the opposite side of the load that is forced to increase due to the impact.

It can be seen that, unlike in the compliant reaction result, the manipulator arm leaves the braking range more quickly under the sudden impact disturbance, allowing the impedance control to become involved more quickly. By comparison with the dropped load that will be bounced without impedance control, the manipulator arm will cushion the impact of dropped load and transition relatively smoothly to a stable position. As a result, the reaction under sudden impact disturbance can be optimized by performing virtual impedance parameters considering the potential sudden disturbance under different situations.

From the perspective of pressure change, the pressure of the opposite side of the load without impedance control reaches a maximum of 7.0 MPa, which is near the pressure limit of the hydraulic muscle. The maximum pressure under impedance control is less than 5.0 MPa; thus, the potential danger of pressure overload is also effectively reduced.

Conclusion

The stability of a hydraulic muscle actuator is proven to be higher than that of a pneumatic muscle actuator owing to its lower angular velocity and less severe oscillation against sudden load separation or impact disturbance.

Under the proposed impedance control with the braking method, the antagonistic joint driven by hydraulic muscles increases its apparent compliance and decreases apparent damping and inertia during the movement. This reduces possible harm to the operator in collaborative tasks. The antagonistic joint can be easily shifted by the operator (shown in Additional file 1). The experiments show that hydraulic muscles with active impedance control have great potential in implementing soft power robots with sufficient dynamic compliance and stability.

The compliant structure of hydraulic muscles allows the manipulator arm to produce a small range of displacement without active control, and the fluid medium allows the arm to better control the rotation velocity under any condition. These characteristics allow a robot actuated by hydraulic muscles to possibly take a more unique control strategy.

Therefore, we proved that antagonistic joints driven by hydraulic muscles are safer in some cases due to higher stability, and the proposed impedance control that takes advantage of the hydraulic muscles can further improve its dynamic compliance. Power soft robots driven by hydraulic muscles have shown potential to achieve complex collaborative tasks.

The increase in internal pressure caused by oil leakage when the servovalves are closed decreases the accuracy. In future work, over-lapped spool servovalves will be used, and internal pressure will be controlled by a better impedance control strategy. By observing the changes in hydraulic pressure and the motion of the manipulator arm, a disturbance observation can be used to regulate the impedance characteristics for high-accuracy

movements and high safety and compliance when receiving an external force.

Supplementary information

The online version contains supplementary material available at https://doi.org/10.1186/s40648-021-00194-5.

Additional file 1. Introduction movie. Additional file shows the comparisons of hydraulic muscle and pneumatic muscle, and the control effect of proposed impedance control.

Acknowledgements
Not applicable.

Authors' contributions
KS, HN, GE and YF conceived the idea of the study; TI and YF designed and performed research; RS and SO fabricated the artificial muscles used in the work; YF wrote the paper; All authors discussed the results and revised the manuscript. All authors read and approved the final manuscript.

Funding
This work was supported by JSPS KAKENHI Grant-in-Aid for Scientific Research(A) under Grant Number JP18H03760.

Data availability statement
The movie supporting the conclusion of this article is included within its additional file. The datasets used or analysed during the current study are available from the corresponding author on reasonable request.

Competing interests
The authors declare that they have no competing interests.

Author details
[1] Department of Mechanical Engineering, Tokyo Institute of Technology, 2-12-1 Okayama, Meguro-ku, Tokyo 152-8550, Japan. [2] Innovative Project Planning and Promotion Department, Bridgestone Corporation, 3-1-1 Ogawahigashi-cho, Kodaira-shi, Tokyo 187-0031, Japan.

Received: 4 September 2020 Accepted: 6 February 2021
Published online: 08 March 2021

References

1. Caldwell DG, Medrano-Cerda GA, Goodwin M (1995) Control of pneumatic muscle actuators. IEEE Control Syst Mag 15(1):40–48
2. Bicchi A, Rizzini SL, Tonietti G (2001) Compliant design for intrinsic safety: General issues and preliminary design. In: Proceedings 2001 IEEE/RSJ International Conference on Intelligent Robots and Systems. Expanding the Societal Role of Robotics in the the Next Millennium (Cat. No. 01CH37180), vol. **4**, pp. 1864–1869. IEEE
3. Blackburn J, Reethof G, Shearer JL (1960) Fluid power control. Wiley, New York
4. Tiwari R, Meller MA, Wajcs KB, Moses C, Reveles I, Garcia E (2012) Hydraulic artificial muscles. J Intell Mater Syst Struct 23(3):301–312
5. Focchi M, Guglielmino E, Semini C, Parmiggiani A, Tsagarakis N, Vanderborght B, Caldwell DG (2010) Water/air performance analysis of a fluidic muscle. In: 2010 IEEE/RSJ International Conference on Intelligent Robots and Systems, pp. 2194–2199. IEEE
6. Ku KK, Bradbeer R, Lam K, Yeung L (2008) Exploration for novel uses of air muscles as hydraulic muscles for underwater actuator. In: OCEANS 2008-MTS/IEEE Kobe Techno-Ocean, pp. 1–6. IEEE
7. Burdet E, Osu R, Franklin DW, Milner TE, Kawato M (2001) The central nervous system stabilizes unstable dynamics by learning optimal impedance. Nature 414(6862):446–449
8. Hogan, N.: Impedance control: An approach to manipulation: Part i—theory (1985)
9. Xiang C, Giannaccini ME, Theodoridis T, Hao L, Nefti-Meziani S, Davis S (2016) Variable stiffness Mckibben muscles with hydraulic and pneumatic operating modes. Adv Robot 30(13):889–899
10. Slightam JE, Nagurka ML, Barth EJ (2018) Sliding mode impedance control of a hydraulic artificial muscle. In: ASME 2018 Dynamic Systems and Control Conference. American Society of Mechanical Engineers Digital Collection
11. Morita R, Nabae H, Endo G, Suzumori K (2018) A proposal of a new rotational-compliant joint with oil-hydraulic Mckibben artificial muscles. Adv Robot 32(9):511–523
12. Mori M, Suzumori K, Takahashi M, Hosoya T (2010) Very high force hydraulic Mckibben artificial muscle with a p-phenylene-2, 6-benzobisoxazole cord sleeve. Adv Robot 24(1–2):233–254
13. Schulte Jr HF (1961) The characteristics of the McKibben artificial muscle. In: The application of external power in prosthetics and orthotics, Appendix H. National Academy of Sciences-National Research Council, Washington DC, pp 94–115
14. Chou C-P, Hannaford B (1996) Measurement and modeling of Mckibben pneumatic artificial muscles. IEEE Trans Robot Autom 12(1):90–102
15. Vanderborght B, Albu-Schäffer A, Bicchi A, Burdet E, Caldwell D, Carloni R, Catalano M, Ganesh G, Garabini M, Grebenstein M, et al (2012) Variable impedance actuators: Moving the robots of tomorrow. In: 2012 IEEE/RSJ International Conference on Intelligent Robots and Systems, pp. 5454–5455. IEEE

Publisher's note